

*Recent Progress Designing Compact
Superconducting Final Focus Magnets for the ILC*

Brett Parker

Presented at the Nanobeam 2005 Conference
Kyoto, Japan
October 17-21, 2005

March 29, 2006

Superconducting Magnet Division

Brookhaven National Laboratory

P.O. Box 5000
Upton, NY 11973-5000
www.bnl.gov

Notice: This manuscript has been authored by employees of Brookhaven Science Associates, LLC under Contract No. DE-AC02-98CH10886 with the U.S. Department of Energy. The publisher by accepting the manuscript for publication acknowledges that the United States Government retains a non-exclusive, paid-up, irrevocable, world-wide license to publish or reproduce the published form of this manuscript, or allow others to do so, for United States Government purposes.

This preprint is intended for publication in a journal or proceedings. Since changes may be made before publication, it may not be cited or reproduced without the author's permission.

DISCLAIMER

This report was prepared as an account of work sponsored by an agency of the United States Government. Neither the United States Government nor any agency thereof, nor any of their employees, nor any of their contractors, subcontractors, or their employees, makes any warranty, express or implied, or assumes any legal liability or responsibility for the accuracy, completeness, or any third party's use or the results of such use of any information, apparatus, product, or process disclosed, or represents that its use would not infringe privately owned rights. Reference herein to any specific commercial product, process, or service by trade name, trademark, manufacturer, or otherwise, does not necessarily constitute or imply its endorsement, recommendation, or favoring by the United States Government or any agency thereof or its contractors or subcontractors. The views and opinions of authors expressed herein do not necessarily state or reflect those of the United States Government or any agency thereof.



RECENT PROGRESS DESIGNING COMPACT SUPERCONDUCTING FINAL FOCUS MAGNETS FOR THE ILC*

B. Parker[#], BNL, Upton, NY 11790, U.S.A.

Abstract

QD0, the final focus (FF) magnet closest to the interaction point (IP) for the ILC 20 mr crossing angle layout, must provide strong focusing yet be adjustable to accommodate collision energy changes for energy scans and low energy calibration running. But it must be compact to allow disrupted beam and Beamstrahlung coming from the IP to pass outside into an independent instrumented beam line to a high-power beam absorber. The QD0 design builds upon BNL experience making direct wind superconducting magnets. We present test results for a QD0 magnetic test prototype and introduce a new shielded magnet design, to replace the previous side-by-side design concept, that greatly simplifies the field correction scheme and holds promise of working for crossing angles as small as 14 mr.

PROGRESS BEFORE SNOWMASS'05

An initial compact superconducting magnet design for a 20 mr crossing angle configuration for the NLC FF was developed shortly after Snowmass'02[1-4]. The design drew upon direct wind magnet experience the HERA-II and BEPC-II Luminosity upgrades[5,6]. Field strengths of the compact superconducting magnets are adjustable to accommodate energy and optics changes and the magnets fit within the original NLC permanent magnet solution space envelope.

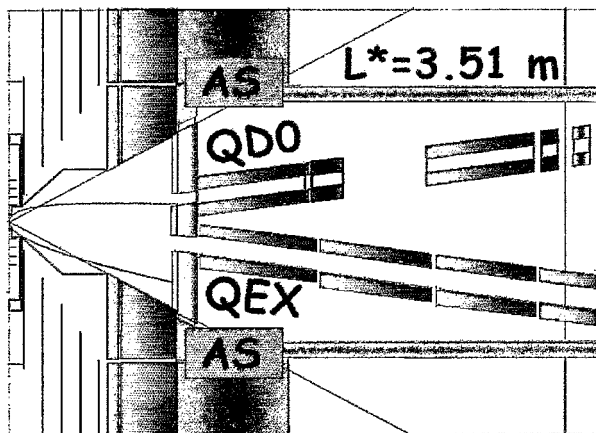


Figure 1. Plan View Schematic of Side-by-Side IR Layout (Obsolete). Disrupted beam from IP goes outside QD0 into the extraction line.

*This manuscript has been authored by Brookhaven Science Associates, LLC under Contract No. DE-AC02-98CH1-886 with the U.S. Department of Energy. The United States Government retains, and the publisher, by accepting article for publication, acknowledges, a world-wide license to publish or reproduce published form of this manuscript, or allow others to do so, for the United States Government purposes.

[#]parker@bnl.gov

The initial direct wind design was limited in that the inner coil layers used single-strand superconducting wire rather than seven-strand round cable used for the main HERA-II and BEPC-II magnets since we had never wound such small bend radius patterns before. But seven-strand cable has an advantage that less dead space is taken up by insulation and other materials so a higher effective engineering current density is possible with cable than single-strand coil windings.

Thanks to recent direct wind research and development, we now wind much tighter bend radius coil patterns using seven-strand cable[7,8]. This advance, along with a change from 4.5°K supercritical liquid He to 1.9°K superfluid He-II cooling, makes the side-by-side magnet scheme, shown in Figures 1 and 2 viable. Here the incoming and extraction beamline magnets start at the same L^* and the required superconducting coil thicknesses are thin enough that the cold masses can be housed in separate cryostats. While starting the extraction beam line close to the IP is helpful in maximizing extraction line acceptance, the main benefit of the side-by-side configuration is for the extraction line where it permits local compensation of the external field generated outside QD0.

We wound and tested a short QD0 prototype, QT, in order to demonstrate that we could meet the ILC QD0

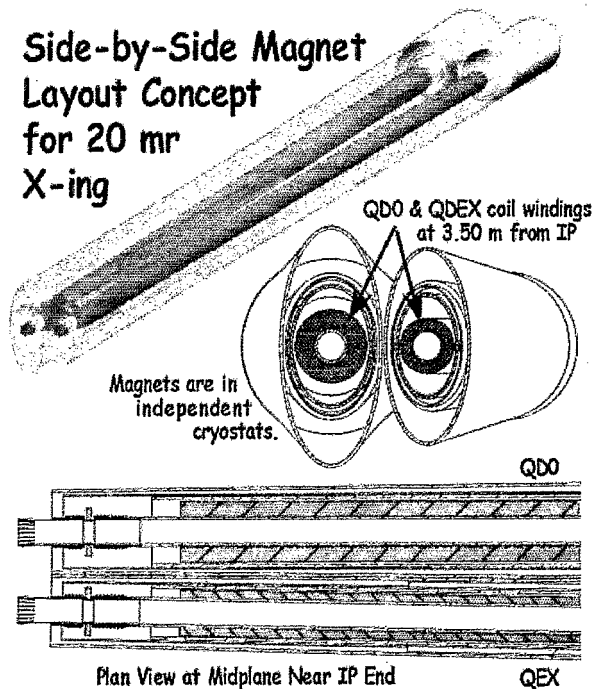
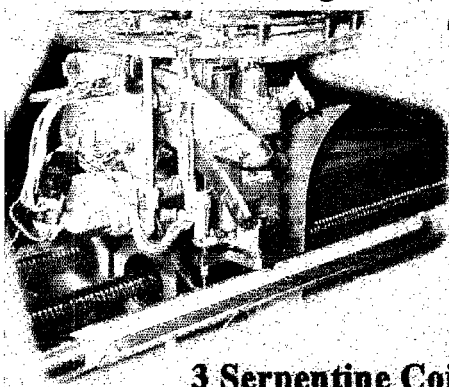
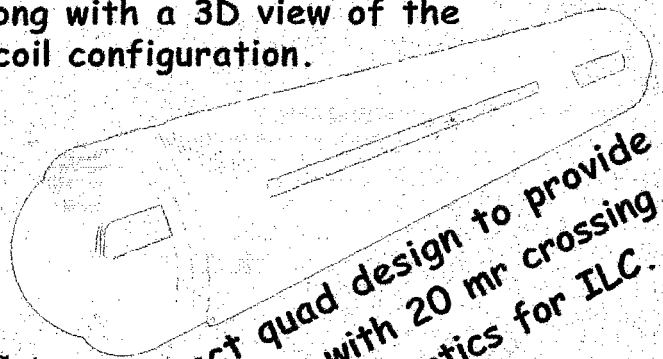


Figure 2. The Side-by-Side Magnet Concept for 20 mr Crossing Angle (Obsolete). Same L^* for extraction line enables partial compensation of QD0 external field.

Start of winding for ILC QD0 Prototype Test Magnet, QT, along with a 3D view of the coil configuration.



3 Serpentine Coil Sets Giving 6 Cable Layers



Compact quad design to provide 140 T/m with 20 mm crossing angle optics for ILC.

Figure 3. Winding the Short QD0 Magnetic Test Prototype, QT, and CAD Model of Final Six Layer Quadrupole Coil Pattern. QT production is complete along with warm field harmonic measurements. Quench testing was performed in an existing BNL dewar at 4.3 to 3.0° K temperature, 1 to 10 A/s ramp rates and solenoidal background fields up to 6 T. design requirements of 20 mm clear full aperture and 140 T/m operating gradient in the presence of a 3 T solenoidal background field. Figure 3 shows the start of QT coil winding along with full final coil structure. QT was produced in three winding steps as Serpentine style dual-layer coil sets A, B and C, for a total of six cable layers[8]. Before winding was complete warm magnetic measurements were performed and the results were used to make minor pattern corrections to the final coil set C.

The chosen 380 mm QT coil length is a compromise between it being long enough to accurately measure central “body” harmonics separately from the field harmonic contribution of each end and it being short enough to fit inside an existing laboratory dewar test setup with an 8 T solenoid. We powered QT in the presence of a background solenoidal field to simulate the impact of the detector solenoid on QD0 performance both in terms of total field on the conductor and the extra internal coil forces due to field interactions at the coil ends.

QT field measurement results are summarized in Table 1. During QT production we learned to wind even tighter bend radius patterns which let us fit more turns. We were also able to slightly decrease interlayer radial spacing for a net 7% increase in transfer function.

Table 1. QT Measured Integral Field Quality. Harmonics are expressed in “units,” a part in ten-thousand, at a reference radius of 5 mm. Numbering convention: N=3 is sextupole. Values less than 0.01 omitted. ILC QD0 design goal has all harmonics less than 10 units at this radius.

Harmonic Number	Coils A+B+C	
	Normal	Skew
T.F. (T/m/kA)	210.7	—
3	0.19	0.43
4	-0.03	1.49
5	-0.20	0.18
6	0.17	0.09
10	-0.26	0.01

tighter bend radius patterns which let us fit more turns. We were also able to slightly decrease interlayer radial spacing for a net 7% increase in transfer function.

Even though ILC field uniformity requirements for QD0 are fairly loose, 0.1% at 5 mm reference radius which corresponds to 10 units in Table 1, the QT coil radius is five times smaller than that of HERA-II for which we had experience. Thus we were interested to see what level of uniformity could reasonably be achieved by adjusting the winding pattern of the last coil set.

Based upon warm measurements done after coil set B was wound, without final tuning we would have expected to see some harmonics as large as 3 units. But with the exception of the skew-octupole, the correction made with coil set C brought all integral harmonics to well below 1 unit; for the skew-octupole a wrong sign correction was input and the harmonic error that should have ended up below 1 unit instead increased to 1.5 units. As expected with Serpentine style coil patterns, the measured integral harmonics tracked the central “body harmonics” very well[9]. Since QT is one-sixth QD0’s length, it has greater end harmonic sensitivity than QD0. So we anticipate no real difficulty in producing FF magnets that meet the 10 unit ILC QD0 field requirements.

Figures 5 and 6 show QT being prepared for cold



**L_{coil} = 380 mm
G_{op} = 140 T/m
I_{op} = 664. A
Harmonics were adjusted using final coil set “C”**

Figure 5. Completed QT Prototype Being Prepared for Vertical Cold Testing. During production we learned to decrease turn spacing and bend radius for a 7% transfer function gain.

testing by adding voltage tap and spot heater diagnostics and attaching QT's leads to current lead feedthroughs. QT was tested with a background field solenoid housed inside in a small laboratory test dewar. The solenoidal field profile is plotted in Figure 6. Testing was performed for various temperature (4.2 to 3.0 °K), ramp rate (1 to 10 A/s) and background field (0 to 6 T) combinations.

QT reached conductor short sample after a single training quench. At 10 A/s ramp rate QT quenched close to 85% (six-sevenths) of short sample due to well known lack of current sharing with center conductor. The 6-around-1 cable used for QT is not intended for fast ramping since the central conductor "drops out" due to its not being transposed with the outer 6 conductors. Slow ramp rate quench results are summarized in Table 2. QD0 is specified to reach 140 T/m in a 3 T background field when cooled to 1.9 °K and QT exceeded this gradient by 13% at 3 T while at an elevated operating temperature of 4.3 °K. QT almost reached operating gradient in a 4 T, background field at 4.22 °K.

To test at lower temperature we lowered the helium dewar pressure via vacuum pumping. Unfortunately such pumping causes the helium level inside the dewar to drop significantly. Because QT had to be "long" to make accurate body harmonic measurements (enough straight section length to get harmonics of the central 254 mm via subtraction of rotating coil readings at two positions) the helium level fell below the current leads around 2.5 °K. The lowest test temperature we took quench data with simple pumping setup, i.e. no λ -plate, was 3.0 °K. In order to avoid running at excessively high current we increased background field to 6 T. Such an increased background field still gives large Lorentz forces in the coil ends but lets us remain below dangerous current

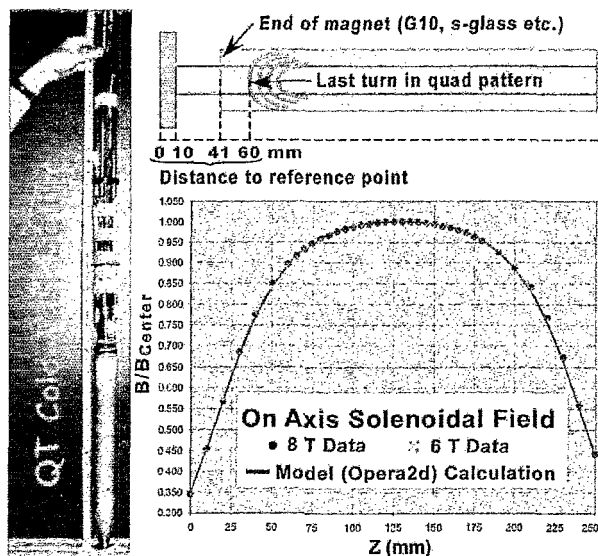


Figure 6. Quench Testing with an Existing Small Dewar and 8 T Solenoid. Solenoid field distribution was modeled and compared to measured (on-axis) data. Off-axis behavior (B_z , B_r) was then calculated to determine high field points in the QT prototype during testing.

Table 2. Summary of Slow Ramp Quench Results (i.e. less than 10 A/s where current sharing of central conductor is not a significant issue). Note: ILC QD0 operational target is 140 T/m gradient in presence of 3 T solenoidal background field while cooled with superfluid He-II @ 1.9°K. These data scale to 232 T/m under proposed ILC operating conditions for operation at 60% short sample.

Background Solenoid (T)	Temp (°K)	Gradient (T/m)
3	4.30	158
4	4.22	139
5	4.22	134
6	3.00	137

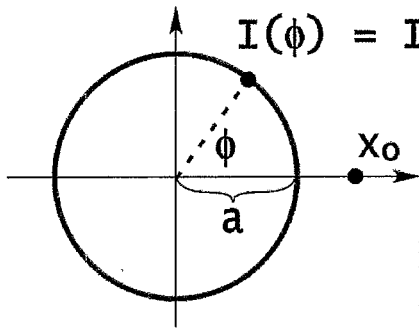
levels where quench protection is an issue. At 3.0 °K and 6 T background, QT reached 137 T/m. When this result is scaled to 1.9 °K and 3 T background field QT should reach 232 T/m (1100 A). So the nominal working point is at 60% of predicted short sample. In future work we plan to test a shorter ILC prototype that should enable data acquisition at lower temperature with the same test setup.

DEVELOPMENTS AFTER SNOWMASS'05

The proceeding discussion summarizes the compact superconducting magnet design status just before the Snowmass'05 meeting. During Snowmass many issues were discussed and in particular the detector groups wanted to know what the minimum crossing angle is for which the compact superconducting could still be used to retain the main advantages of the 20 mr layout, i.e. truly independent incoming and extraction beamlines for which upstream and downstream beam diagnostic sections could be provided. Referring to the side-by-side configuration shown in Figure 2, one approach to reducing the beamline separation is to eliminate space for the double cryostat and put both cold masses in a common cryostat. But the mutual external fields present at both beamlines increases very rapidly with decreasing separation. This forces us to use stronger correction coil windings which then generate their own stronger external fields which have to be compensated. The "cross talk" between the two beamlines increases dramatically with reduced separation and optimization of the correction/compensation scheme becomes more difficult.

It is interesting to consider what occurs when the first extraction line magnet, labeled QDEX in Figure 2, is replaced by a bare beam pipe. The external field generated by QDEX is gone but so is the opportunity for local compensation of QD0's external field unless we add an active shield coil.

As outlined in Figure 7 and shown implemented, for realistic QD0 coil parameters in Figure 8, active shielding can have minimal impact on QD0 performance when the average inner and outer coil radii, a_1 and a_2 , are



Quadrupole $m=2$

$$G^{out} = G^{in}(a/x_0)^4$$

$$B^{out} = -(G^{in}a)(a/x_0)^3$$

For coils 1 & 2 to have external field shielded...

$$\text{We need: } I_2 = (a_1/a_2)^2 I_1 \text{ for } G^{net} = G_1[1 - (a_1/a_2)^4]$$

Figure 7. Criteria for Field Cancellation at Point X_0 Outside Two Concentric Nested Current Distributions. The case of quadrupole external field shielding is emphasized. For a pure quadrupole its external field can be eliminated while retaining a significant net inside gradient, G^{net} , thanks to the fourth power scaling with average coil radius.

sufficiently different. Our proposed QD0 active shield design brings only a 5% increase in excitation current.

With reduced external field we can place the extraction beam pipe close to the outer shield. In Figure 9 we plot the external field seen by extracted beam with this new solution as a function of distance to the IP, Z_{IP} , for QD0 L^* of 3.51 m but now done for a 14 mr crossing angle. Near the middle of QD0 the cancellation is nearly perfect while at each end there is a small residual field. The 2D approximation outlined above breaks down near the coil ends and the IP end separation is smallest yielding the largest residual field there.

We manufactured a shield coil for the QT prototype with the coil layout shown in Figure 10 that could just fit inside our test solenoid in order to test the active shielding

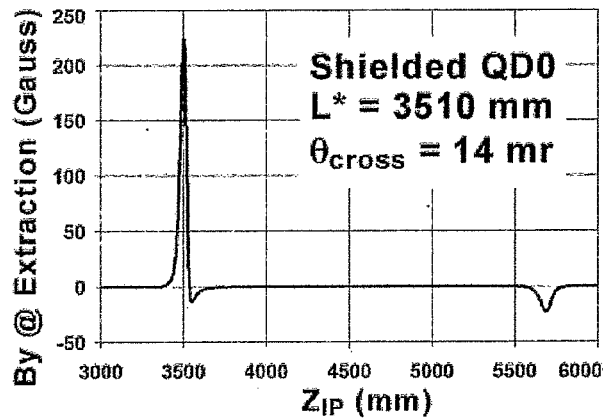


Figure 9. Field Seen Outside an Actively Shielded QD0 Magnet at Extraction Beamline.

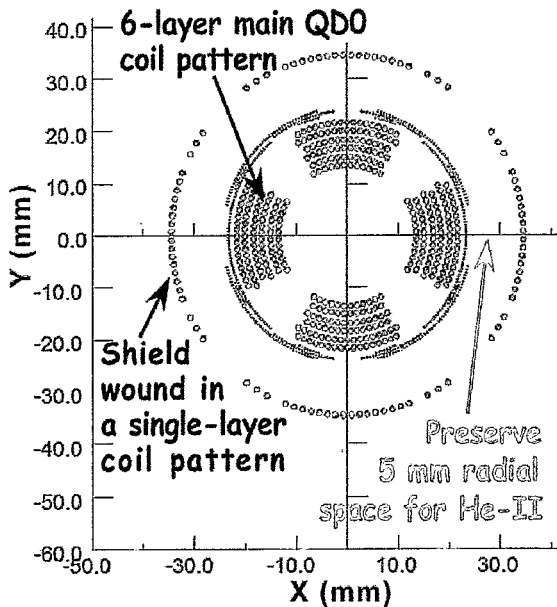


Figure 8. Actively Shielded QD0 Design Compatible with 14 mr Crossing Angle. The inner and outer coils are wound on separate support tubes (not shown) with 5 mm space left inside the outer support tube for He-II cooling. Running both coils at ≈ 700 A gives 148 T/m from the inner coil and -8 T/m from outer for 140 T/m net gradient.

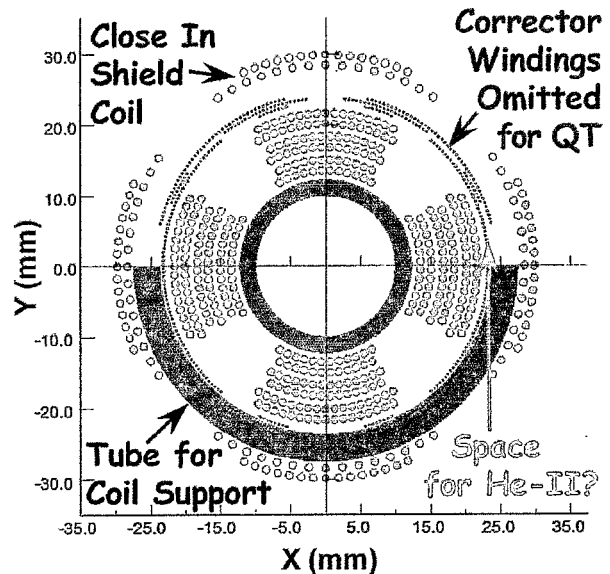


Figure 10. Shield Coil Design for QT, the QD0 Magnetic Prototype. For 748 A, G_{in} is 157.5 T/m while G_{outer} is -17.5 T/m for net 140 T/m gradient. There is limited space for He-II between QD0 and the support tube that is produced by omitting the QD0 correction coil windings.

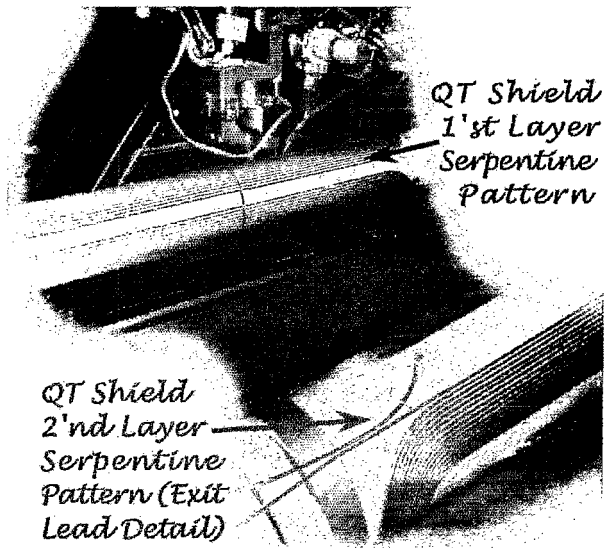


Figure 11. Production of QT Two-Layer Active Shield.

concept. Because this QT shield coil is pulled closer in, a greater number of shield turns are required.

Both layers of the QT shield coil are pictured during winding in Figure 11 and assembled with the original QT prototype in Figure 12. Due to the short time span between the end of Snowmass'05 and the present Nanobeam'05 conference, we produced the shield coil support tube using existing stock with wall thickness about 1 mm thicker than desired. The correction windings shown in Figure 10 were omitted in order to provide some space for helium cooling and not to delay production.

This QT active shield coil illustrates issues that arise with bringing the shield closer in to QD0 than the amount budgeted in Figure 8 (i.e. if one tries to reduce the crossing angle below 14 mr). An obvious impact of pulling the closer in similar to the QT shield design is that the current now has to rise to 748 A in order to reach 140 T/m which is a 13% increase compared to a bare QD0. The associated reduction in operating margin is troubling but is not the most important impact.

In Figure 10 we see that the space available for direct He-II cooling of such an inner coil package is quite tight. While superfluid helium can penetrate small gaps, the amount of heat that can be removed through a long cooling section depends critically on available space. Since QD0's beam related energy deposition occurs primarily on its innermost structure, the annular space available for He-II in contact with the inner coils determines the temperature profile along QD0's length.



Figure 12. QT Magnet Installed Inside its Two-Layer Active Shield.

The outer radius shown in Figure 8 of the 14 mr crossing angle compatible shield coil is only a few millimeters larger than that shown for QT in Figure 10 but includes 5 mm space inner helium cooling while QT has essentially none. Some of the outer radial space that could have been gained by pulling the QT shield closer in was instead lost due to doubling the shield coil thickness.

However even with its tight design space constraints, the shield coil was quite successful in reducing the QT external field. Magnetic measurements made with a rotating coil parallel to the QT axis and almost touching the shield coil outer surface show that the integrated external field is reduced by a factor of 22 when the QT and shield coils are powered in series. This result gives us confidence that active shielding should work very well for the proposed 14 mr crossing angle shield configuration. The field at the shield coil is already smaller and the cancellation is not as delicate as for QT. For QD0 we foresee providing a small trim current across the shield coil for fine tuning capability, but our QT active shielding test result suggests that this precaution may not really be necessary. We will make further tests when a full length actively shielded QD0 prototype is finally produced.

Figure 13 shows one possible realization of an actively shielded QD0 for 14 mr crossing with a tapered extraction beam pipe almost touching the shield coil at the IP end. Note that here the QD0 coils and the extraction line beam pipe share a common He-II volume in a cold mass and are supported in a single cryostat. Important features, such as the IP end warm-to-cold beam pipe transition and connection to a helium supply line with control valves and current leads, are shown but may be modified as the design matures.

Preliminary designs have been worked out for all the compact superconducting magnets needed to implement the 14 mr crossing angle IR. A schematic representation of the compact superconducting magnets on one side of the IR for 14 mr crossing angle and L^* of 3.51 m is shown in Figure 14. Note that with the proposed scheme the first extraction line magnet, QDEX1A, starts past QD0 at 6 m. The actively shielded coil layout for QDEX1A is shown in Figure 15. It is important that the stray field from QDEX1A seen at the incoming beam

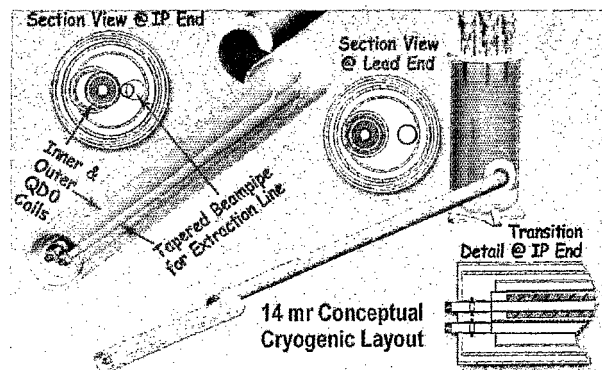


Figure 13. CAD Schematic of QD0 Cryogenic Assembly. Tapered extraction line beam pipe is along side QD0 and shares a common He-II volume inside a common cryostat.

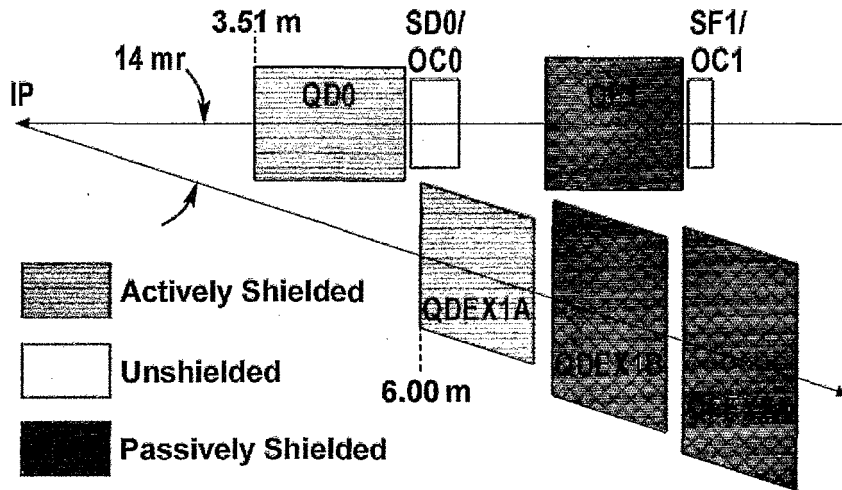


Figure 14. Schematic Representation of the Compact Superconducting Magnets on One Side of the IP (Plan View). Note that distances are compressed along the incoming beamline and this has the effect of distorting the apparent shape of magnets that are not parallel to this direction. Sizes shown for the various magnet boxes are intended to give a comparative indication of the various magnets' sizes. Coding is as indicated: actively shielded (red with horizontal banding), unshielded (plain yellow) and passively shielded (blue hatched). Passive shielding is used for magnets well outside the detector solenoid where they have thin magnetic yokes that reduce their external fields. Unshielded magnets are either weak correction coils or have sufficiently high multipolarity that their external fields die off rapidly.

location be small since too large a field, even with a zero net integral, could cause too much synchrotron radiation and impact luminosity by spoiling the beam's emittance. Fortunately even though QDEX1A has a larger average coil radius than QD0, so its fringe field ought to extend further out, it is weaker than QD0 and the beam separation is greater at QDEX1A, so residual stray field seen by the incoming beam, shown in Figure 16, is small.

With direct wind magnet production it is natural to co-wind different magnet coils in concentric layers (instead of longitudinal segmentation). For instance by making an

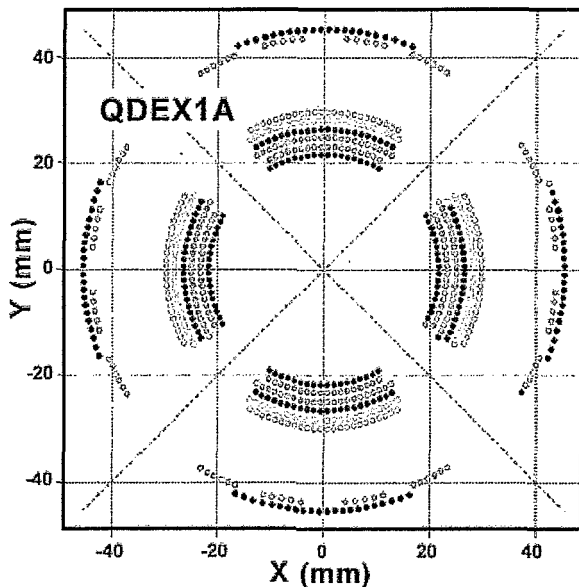


Figure 15. Actively Shielded QDEX1A Design for 14 mr Crossing Angle. Inner and outer coils are wound on separate support tubes. For 730 A, G_{in} is 93.8 T/m while G_{outer} is -10.5 T/m for net 83.3 T/m gradient.

octupole magnet, such as OC0, longer we can achieve its required integrated field strength with fewer coil layers and the resulting coil package is itself more efficient because the average coil radius is smaller. Thus we can combine the original space allocation for the SD0 sextupole with OC0 and co-wind them in the pattern shown in Figure 17.

The octupole, being the higher multipolarity, is most favorably wound first on the support tube since this dramatically reduces its field strength at the conductor inner surface. But then the sextupole radial start point goes outward and for a fixed number of coil layers the sextupole ends up being weaker. However, since the sextupole is now longer, the required integrated field strength is still attained without increasing the excitation

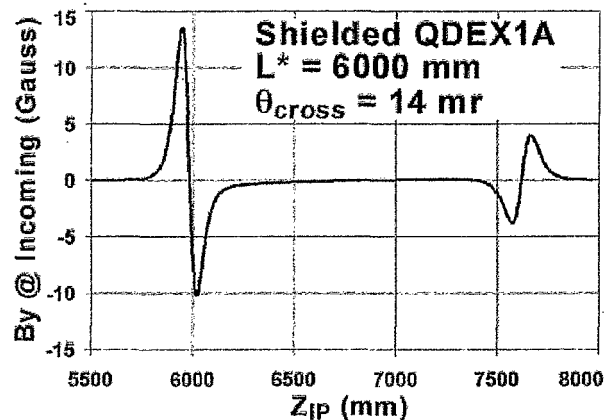


Figure 16. Stray Field Seen Outside QDEX1A at the Incoming Beamline. Stray field at the incoming beam location is more critical there than at the extraction line; so we seek to reduce it as much as possible, both in an integral sense and locally, to avoid large field excursions.

Table 3. Parameter Summary for the SD0, OC0 and Correction Windings in Their Common Coil Package.

Design of 6-Oct-2005	L _{tot} (mm)	T.F @ cent	I.T.F	L _{mag} (mm)	I _{op} (A)	B or Gradient Units	B @ 10 mm (T)	Ext' @ 85 mm	B @ 85 mm (Gauss)
octupole	716 + 20	1.901E+03	1.346E+03	708.0	79	1.50E+05 T/m ³	0.150	3.10E-06	0.5
sextupole	716 + 20	8.462E+00	5.923E+00	700.0	709	6.00E+03 T/m ²	0.600	1.34E-02	81
skew sextupole	716 + 20	3.814E+00	2.651E+00	695.2	79	3.00E+02 T/m ²	0.030	4.07E-02	12
dipole (hor)	716 + 20	1.165E-03	7.610E-04	653.0	86	1.00E-01 T	0.100	9.31E+02	93
dipole (vert)	716 + 20	7.681E-04	4.997E-04	650.6	91	7.00E-02 T	0.070	9.74E+02	68

current. One consequence of co-winding different multipolarity coils with the same pattern length is that they naturally end up with different magnetic lengths. In Table 3 OC0 and SD0 show the same 716 mm coil pattern length but their respective magnetic lengths, 708 and 700 mm, differ.

The additional corrector windings shown in Figure 17, and parameterized in Table 3, are:

- skew-sextupole (specified to have 5% of main sextupole integrated strength for generating an effective sextupole field rotation)
- dipole and skew-dipole windings (used to shift the magnetic center).

These correction coil windings are useful because the SD0/OC0 package is wound on a continuation of the QD0 coil support tube and it is not practical to move or rotate this package independently inside a cryostat.

In order to compare the stray field generated by these elements at the extraction beamline, we display in the last column of Table 3 the field contribution from each one when operated at maximum specified operating current and at the minimum beam separation. We see that even though the dipole and skew-dipole corrector fields are much weaker than the sextupole at the 10 mm beam pipe inner radius, if these correctors were to be run up to full current they would contribute almost as much as the sextupole to the external field seen at the extraction line because their external fields fall off much more slowly

(combination of larger average radius and dipole's $1/r^2$ dependence compared to sextupole's $1/r^4$). But note that even though the octupole field magnitude, is one-quarter the sextupole field inside at 10 mm radius, the octupole contribution is negligible at the extraction beamline (octupole has smaller coil radius and $1/r^5$ dependence). Finally the skew-sextupole is 5% of the main sextupole inside the aperture but 15% of the main sextupole outside (skew-sextupole radius is larger and same r-dependence).

The SD1/OC1 coil package has the same coil cross section as SD0/OC0 but its stray field seen at the extraction line will be much smaller because:

- the beamline separation at SD1/OC1 is greater,
- and the passive shielding keeping QFEX2A stray field from the incoming beamline also works to keep SD1/OC1 stray field from reaching the extraction line.

Magnets which are beyond QDEX1A are comfortably outside the experimental detector solenoid where we can switch from active shielding via reverse polarity coils to passive shielding with magnetic materials. Unlike active shielding which reduces magnetic strength, passive shielding adds to the strength and works for all the field multiplicities that are present (i.e. on correction coils as well as with the main magnets).

The cross section of a passively shielded magnet, QF1, is shown in Figure 18. For passive shielding we use a magnetic yoke shell that is placed at large enough radius

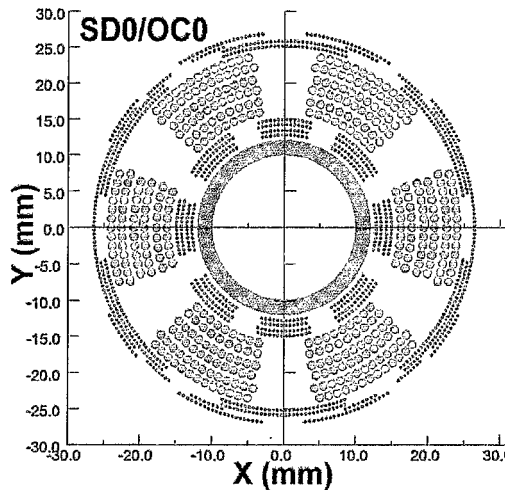


Figure 17. SD0/OC0 Common Coil Package. The SD0 (sextupole) and OC0 (octupole) coils are co-wound on a support tube and have the same physical length. First OC0 is wound with 4 layers of single stand wire followed by 6 cable layers for SD0. Atop this are skew-sextupole, dipole and skew-dipole correction coil windings.

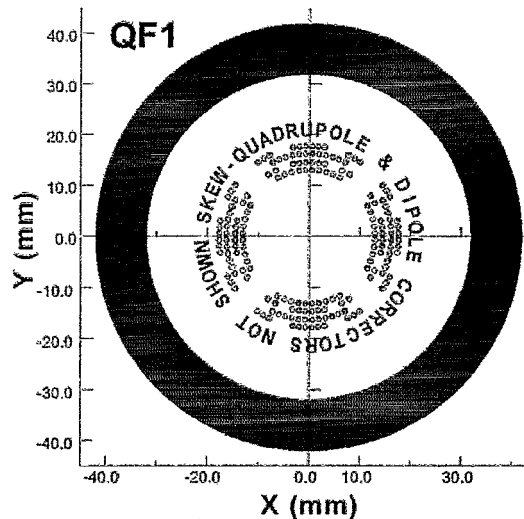


Figure 18. A Passively Shielded QF1 Magnet that is Suitable for 80 T/m Operation. A thin cold magnetic yoke surrounds the QF1 coil (both containing stray field and increasing transfer function). This design has space inside the yoke for He-II cooling in contact with the inner coil

Table 4. Incoming Beamline Magnet Package Summary.

Package Name	Multipole Type	Shield	Winding Type	Total # Layers
QD0	Main Quadrupole	Yes	Cable	6
	Dipole	No	Wire	1
	Skew-Dipole	No	Wire	1
	Skew-Quadrupole	No	Wire	1
	Shield Quadrupole	—	Cable	1
SD0	Octupole	No	Wire	4
	Sextupole	No	Cable	6
	Skew-Sextupole	No	Wire	2
	Dipole	No	Wire	1
	Skew-Dipole	No	Wire	1
QF1	Quadrupole	Yes	Cable	4
	Dipole	Yes	Wire	1
	Skew-Dipole	Yes	Wire	1
	Skew-Quadrupole	Yes	Wire	1
	Magnetic Yoke	—	—	1
SF1	Octupole	No	Wire	4
	Sextupole	No	Cable	6
	Skew-Sextupole	No	Wire	2
	Dipole	No	Wire	1
	Skew-Dipole	No	Wire	1

to remain unsaturated. With the shell being at large radius it has only minimal impact on field quality and has little sensitivity to relative centering errors between the coils and shield. Note it is still important to provide space for He-II cooling in direct contact with the coil surface inside the passive shielding shell.

Since QF1 is not impacted by the detector solenoid field, has a lower operating gradient of 80 T/m and passive shielding that boosts its gradient, its conductor requirements are greatly relaxed compared to QD0 and is wound with fewer cable layers. QF1 will still have the same compliment of skew-quadrupole, dipole and skew-

Table 5. Extraction Beamline Magnet Package Summary.

Package Name	Multipole Type	Shield	Winding Type	Total # Layers
QDEX1A	Main Quadrupole	Yes	Cable	6
	Dipole	No	Wire	1
	Skew-Dipole	No	Wire	1
	Skew-Quadrupole	No	Wire	1
	Shield Quadrupole	—	Cable	2
QDEX1B	Quadrupole	Yes	Cable	6
	Dipole	Yes	Wire	1
	Skew-Dipole	Yes	Wire	1
	Skew-Quadrupole	Yes	Wire	1
	Magnetic Yoke	—	—	1
QFEX2A	Quadrupole	Yes	Cable	6
	Dipole	Yes	Wire	1
	Skew-Dipole	Yes	Wire	1
	Skew-Quadrupole	Yes	Wire	1
	Magnetic Yoke	—	—	1

dipole correction coils (not shown in Figure 18) as QD0. For QF1 its passive shielding has two additional benefits:

- external fields generated by the correctors are also shielded from the extraction beamline
- and the shield prevents outside stray fields from reaching the incoming beamline.

For completeness the designs for the remaining passively shielded extraction line magnets are shown in Figure 19. Summaries for all the coil packages are given in Tables 4 and 5. The extraction line QDEX1B and QFEX2A magnets are similar to QF1; however, in order to reduce energy loss due to disrupted beam coming from the IP their apertures must be increased. Given the tight transverse separation between the incoming and extraction beamlines, shown in Figure 14 and the need not to saturate the QDEX1B and QFEX2A magnetic yokes (avoid higher external field from saturated yokes), the

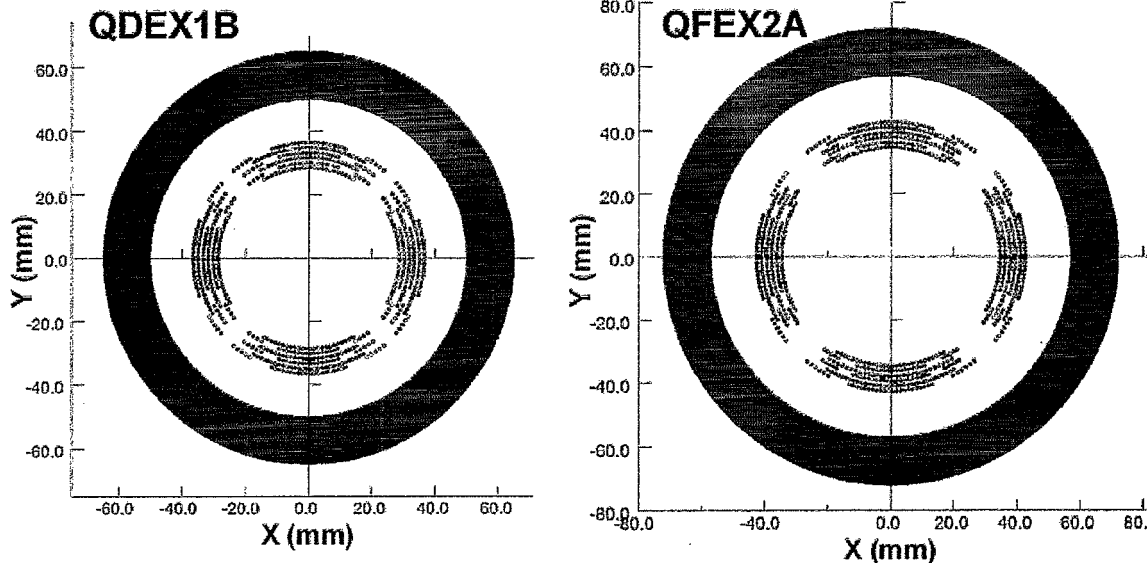


Figure 19. Passively Shielded Designs for the Final Two Extraction Line Superconducting Magnets QDEX1B and QFEX2A. As we go further from the IP the extraction line aperture must grow in order to keep energy deposition manageable and therefore the quadrupole field strength drops from 50 T/m for QDEX1B to 40 T/m for QFEX2A.

Table 6. Coil Package Physical Parameters for the 14 mr Crossing Angle Layout. L_{pat} is the coil pattern length, R_{opt} the beampipe inner radius (half-aperture) and R_{outer} the outer package radius (for coil or yoke as appropriate).

Package Name	L_{pat} (mm)	R_{opt} (mm)	R_{outer} (mm)
QD0	2220	10	36
SD0	716	10	28
QF1	2020	10	42
SF1	366	10	28
QDEX1A	1674	18	46
QDEX1B	1680	24	62
QFEX2A	1686	30	72

QDEX1B and QFEX2A magnetic fields at their inner apertures are set to be less than 1.2 T.

Relevant physical parameters of the coil package and yoke sizes used for the 14 mr layout are given in Table 6. Note that these data are useful for deriving a lower limit for the crossing angle with the present design even if L^* were to be increased by 1 m from 3.51 to 4.51 m. With the present 14 mr layout, the QF1 and QDEX1B yokes are close to touching at 7.9 m with (7900*0.014-42-62) or 6.6 mm. With L^* increased to 4.51 m, we find that it would take a crossing angle of 12.4 mr to maintain this same spacing at the new 8.9 m location and this crossing angle is more than the value of 11 mr estimated from simple L^* scaling (i.e. 3.51/4.51*14 mr).

SUMMARY

We have shown how to use BNL direct wind coil production techniques, originally developed for the HERA-II and BEPC-II Luminosity Upgrades, for making compact superconducting ILC FF magnets compatible with L^* of 3.51 m and 14 mr total crossing angle. Some critical milestones were:

- learning to wind small bend radius cable coil patterns on small diameter coil support tubes (increased engineering current density)
- adoption of He-II cooling (better performance)
- and the development of active and passive external field shielding configurations (to eliminate beamline magnet field cross talk).

A short actively shielded QD0 prototype, QT, was produced and tested and QT performance exceeded ILC field quality and quench performance requirements. Even with the somewhat compromised shield design that had to be adopted to fit test dewar space limits, the QT active shield performed very well and reduced QT's integrated external field on contact by 22 fold.

In future work we will integrate heating elements directly into the body of a test coil prototype in order to directly measure the energy required to quench compact superconducting magnets under ILC operating conditions.

With preliminary coil and yoke dimensions now in hand we are proceeding with a cryogenic design that integrates the 14 mr layout magnets in a common cryostat. Finally we plan to produce a full length prototype to be housed and supported in a full cryostat in order to be able to investigate vibration and active stabilization issues.

REFERENCES

- [1] B. Parker, "Superconducting Magnet Issues," ICFA Beam Dynamics Workshop on Nanometer-Size Colliding Beams, Nanobeam 2002, Lausanne Switzerland, September 2002, <http://www.bnl.gov/magnets/Staff/Parker/ParkerNano2002Talk.pdf>.
- [2] B. Parker, "Superconducting Final Focus Magnet Issues," NLC US Machine Advisory Meeting, November 2002, SLAC, Palo Alto, CA, USA, <http://www.bnl.gov/magnets/Staff/Parker/ParkerMAC7NovTalk.pdf>.
- [3] B. Parker, "The Compact Superconducting Final Focus Doublet Option," American Linear Collider Workshop, Cornell University, Ithaca, NY, USA, July 2003.
- [4] B. Parker, "A review of the BNL Direct-Wind Superconducting IR magnet Experience," 30th Advanced ICFA Beam Dynamics Workshop on High Luminosity e^+e^- Collisions, Palo Alto, CA, USA, October 2003 <http://www-conf.slac.stanford.edu/icfa03/pres/MOP03.pdf> and <http://www-conf.slac.stanford.edu/icfa03/pres/MOP03.mov>
- [5] P. Wanderer, *et.al.*, "Completion of Superconducting Magnet Production at BNL for the HERA Luminosity Upgrade," 17th International Conference on Magnet Technology, MT-17, Geneva, Switzerland, September 2001, http://www.bnl.gov/magnets/magnet_files/Publications/BNL-71432-2003-CP.pdf.
- [6] B. Parker, "The Serpentine Coil Design for BEPC-II Superconducting IR Magnets," Mini-Workshop on BEPC-II IR Design, IHEP, Beijing, P. R. China, January 2004, http://www.bnl.gov/magnets/Staff/Parker/serpentine_review.pdf.
- [7] B. Parker, "Technology Development for Linear Collider Final Focus Quadrupoles with Small-Aperture High-Gradient Superconducting Coils," BNL LDRD Project Number **LDRD-03-014**, 2003.
- [8] B. Parker, *et.al.*, "Compact Superconducting Final Focus Magnet Options for the ILC," 2005 Particle Accelerator Conference, PAC'05, Knoxville, Tennessee, USA, May 2005, <http://accelconf.web.cern.ch/AccelConf/p05/PAPERS/RPPP017.PDF>
- [9] B. Parker and J. Escallier, "Serpentine Coil Topology for BNL Direct Wind Superconducting Magnets," 2005 Particle Accelerator Conference, PAC'05, Knoxville, Tennessee, USA, May 2005, <http://accelconf.web.cern.ch/AccelConf/p05/PAPERS/TOAA010.PDF>.